

Vertical distribution of ^{40}K , ^{232}Th , and ^{137}Cs mass activities in lake sediment (Vransko Lake, Croatia) and their relationship with the source material and sedimentation

H. Fajkovic · I. Lovrencic Mikelic ·
E. Prohic

Received: 26 September 2012 / Published online: 30 November 2012
© Akadémiai Kiadó, Budapest, Hungary 2012

Abstract The goal of the study was to research the relationship between the source rocks and the sediment deposited in the Vransko Lake in the Ravni Kotari area and to study the sedimentation pattern in the lake. Sediment was classified as the sandy silt and the phase analysis showed the presence of the calcite, quartz, micas, and pyrite. It is possible that the anoxic conditions formed in the sediment due to the pyrite presence. Carbonate component predominates in the sediment composition. CaCO_3 mass fractions in the range 72–94% with the mean values in the range 82–88% were determined. ^{40}K mass activities were in the range 31–166 Bq/kg, ^{232}Th in the range 3.1–18 Bq/kg, and ^{137}Cs in the range 0.3–68 Bq/kg. Negative correlations between CaCO_3 mass fractions and radionuclides mass activities were determined. Correlations between the radionuclides mass activities were positive. In the NW part of the lake sedimentation rates of 10.0, 4.1 and 5.0 mm/a were estimated for the 1954–1964, 1964–1986, and the 1986–2010 periods, respectively. At the SE part sedimentation rates for the respective periods were as follows: 8.0, 2.3 and 2.5 mm/a. Average sedimentation rates were 6.4 mm/a for the NW part of the lake and 4.2 mm/a for the SE part. Sedimentation rate in the Vransko Lake varies in time and showed a significant decrease after the

1964. The input of the carbonate and silicate material into the lake is also variable.

Keywords Sedimentation rate · Vransko Lake · Radionuclide · ^{137}Cs · ^{232}Th · ^{40}K · Gamma-spectrometry · Source rock

Introduction

Lake sediments can be used for interpretation of the past conditions and numerous information can be obtained from them. Like other sediments, they serve as an important reservoir of all substances introduced into the environment. Natural and anthropogenic radionuclides can be used to understand processes in the lacustrine environment [1]. One of probably the most frequently used anthropogenic radionuclides for monitoring of the environmental processes is ^{137}Cs [2, 3]. ^{137}Cs is widely used as a marker for sedimentation rate estimations in various aqueous environments including lakes [4–6]. Due to the known time of the intensive ^{137}Cs input into the global atmosphere, it is possible to observe the typical ^{137}Cs distribution pattern in the undisturbed sediments with characteristic peaks of maximum ^{137}Cs mass activities representing the sediment surfaces of the respective years [1, 7]. The first release of ^{137}Cs into the environment was in 1945 during the early nuclear tests but it was not yet globally deposited. Global input of ^{137}Cs into the environment began with high-yield thermonuclear tests during 1952–1954 [8] resulting with a peak of ^{137}Cs mass activity in 1964 [1, 9]. The second globally significant release of ^{137}Cs into the environment was caused by the Chernobyl accident in 1986 [10, 11] resulting with the second characteristic peak, while the latest one occurred in 2011 by the Fukushima Dai-ichi nuclear power plant accident [12].

H. Fajkovic (✉) · E. Prohic
Institute of Mineralogy and Petrology, Faculty of Science,
Horvatovac 95, 10 000 Zagreb, Croatia
e-mail: hanaf@geol.pmf.hr

E. Prohic
e-mail: eprohic@geol.pmf.hr

I. Lovrencic Mikelic
Laboratory for Radioecology, Rudjer Boskovic Institute,
Bijenicka cesta 54, 10 000 Zagreb, Croatia
e-mail: ivanka.lovrencic@irb.hr

^{40}K and ^{232}Th are primordial natural radionuclides and are present in all rocks, sediments and soils [13, 14]. ^{40}K is the only radioactive isotope of the three potassium isotopes. It is one of the most abundant naturally radioactive elements [15] and is usually associated with the clay minerals [16, 17]. Thorium is mostly bound to the terrestrial/detritic material of which it is indicator [18, 19]. It is very insoluble in water and therefore is rapidly scavenged onto settling particles, removed from the water column, and buried into sediment [20]. Since both of these radionuclides are associated with particles, they can be used as sediment tracers to study the origin of the sediment.

The former studies of the Vransko Lake were mostly aimed at determining the geological, hydrological, and hydrogeological setting of the area [21–24]. Only recently Markovic et al. [25] investigated the area of the Vransko polje in order to evaluate anthropogenic influence from agricultural activities on groundwater and soil. No evidence of the previous research of the sedimentation conditions and rates in the lake has been found. The objective of this study was to research the sedimentation conditions in the Vransko Lake, estimate the sedimentation rate in the lake using ^{137}Cs mass activities depth profiles, to determine whether the sedimentation rate is uniform in the whole lake, and to establish the relationship between the material deposited in the lake and the surrounding carbonate and noncarbonate rocks.

Experimental

Vransko Lake, Croatian largest natural lake with an area of 30.2 km², is located in the geographical region of Ravni Kotari (North Dalmatia) between the towns of Zadar and Sibenik (Fig. 1). To avoid the confusion, it is necessary to emphasize that there are two lakes in Croatia called Vransko Lake. One is in the area of the Ravni Kotari and the other is on the Cres Island. Sometimes, wrongly, both of these lakes are referred to as the largest Croatian lakes. Vransko Lake in the Ravni Kotari area is the lake with the largest surface and the lake on the Cres Island is the deepest lake with the maximum depth of 84 m. The investigated lake is a criptodepression with the maximum depth of 5 m and without any significant depth variations. The lake and its surroundings have been declared an ornithological reserve in 1983 and since 1999 it is a nature park. The lake is situated parallel to the coast line, in a Dinaric direction of stretching, i.e. NW–SE. A narrow ridge (800–2,500 m wide and maximum 113 m high) composed of limestone with some dolomites separates the lake from the Adriatic Sea. The initial relief was formed by the end of Pleistocene. The surrounding terrain is built of Cretaceous and Eocene limestones and Eocene flysch (Fig. 1), while the lake bottom and karst poljes are covered with Quaternary deposits of Holocene age [21, 26–28]. The majority of the groundwater flow and the lake watershed are from the direction of Ravni Kotari situated NW of the

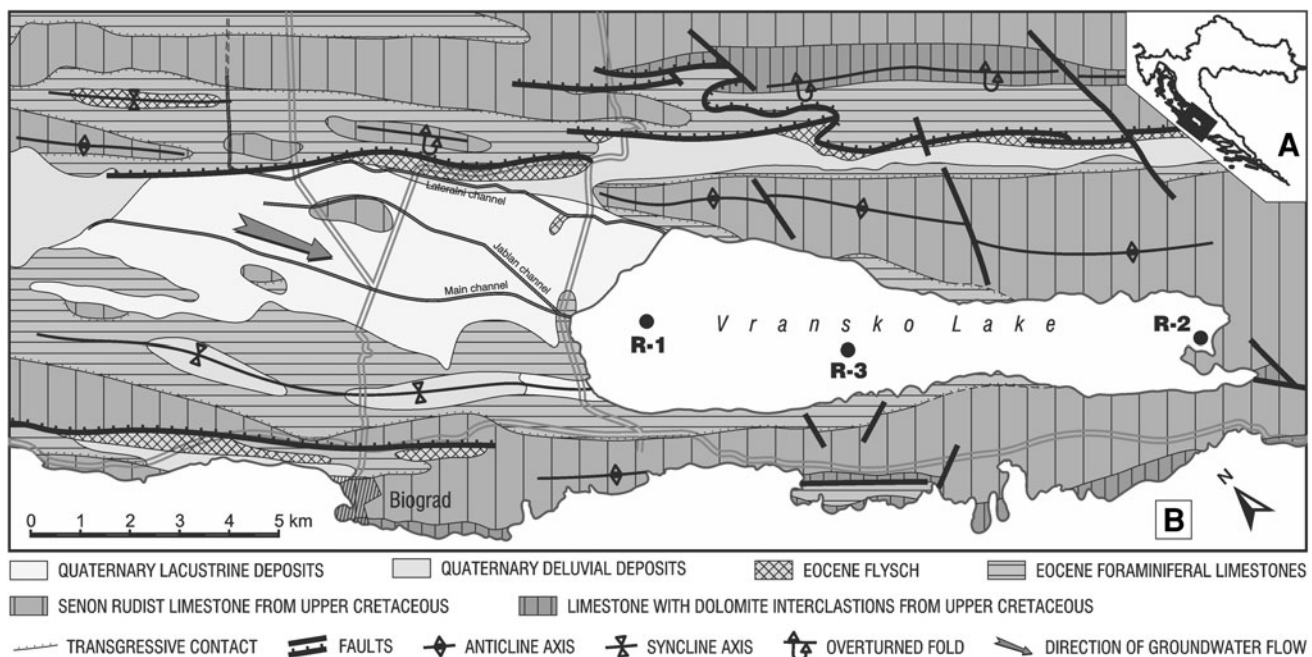


Fig. 1 a Location of the Vransko Lake; b Simplified geological map of the surrounding area and the position of the R-1, R-2, and R-3 sampling stations; (simplified after [21, 27, 28])

Vransko Lake [22, 24, 25] and it is presumed to be the main source of terrigenous material to the lake.

Sediment at three stations in the Vransko Lake (Fig. 1) was sampled in the summer 2010 by scuba diving, using the hand plastic corers. The R-1 station is in the NW part of the lake and it is under higher influence of the watershed, while the R-2 station is more than 11 km further away in the SE part of the lake where the watershed influence is expected to be less pronounced. The R-3 station is located in the middle of the lake, between R-1 and R-2 stations. Sampling location coordinates are: N43°55'57.113", E15°31'33.011" (R-1); N43°51'48.493", E15°37'55.157" (R-2); N43°54'16.74", E15°33'32.737" (R-3). Sediment cores, approximately 30 cm long, were cut into smaller sub-samples of 2 cm in thickness, put in the plastic bags, frozen, and transported to the laboratory.

Prior to performing radiometric analyses, sub-samples were dried at 50 °C until the constant weight, ground in an agate mortar, and homogenized. Plastic counting containers of 125 cm³ volume were filled to the top and firmly sealed. Radiometric analyses of all sub-samples from the R-1 and R-2 stations were performed by gamma-spectrometry technique using a HPGe semiconductor detector with 25.4 % relative efficiency coupled with a multichannel analyzer with 8,192 channels (Canberra Industries). Sub-samples from the R-3 sampling station were not subjected to the radiometric analysis due to the insufficient amount of the collected sediment. Detector resolution was 1.80 keV at 1,332.5 keV line of ⁶⁰Co. Spectra were collected for 80,000 s and analysed by Genie 2000 software (Canberra Industries). ⁴⁰K mass activity was determined through the 1,460.75 keV peak and ¹³⁷Cs mass activity through the 661.66 keV peak. ²³²Th mass activity was determined from the 911.2 keV peak of its ²²⁸Ac progeny. Measurement uncertainties of ⁴⁰K mass activities expressed for 2σ were in the range 11–38 % for all samples, except for two samples of the R-1 sediment core (samples from the depths 34–36 cm and 36–38 cm) for which the uncertainties were 56 % and 52 %, respectively, and for one sample of the R-2 sediment core (sample from the depth 22–24 cm) for which the uncertainty was 55 %. Measurement uncertainties of ¹³⁷Cs mass activities were in the range 7.7–25 % for all samples except for two. One sample was from the R-1 core (sediment depth 32–34 cm) and one from the R-2 core (sediment depth 18–20 cm). The respective uncertainties were 125 % and 63 %. Uncertainties of ²³²Th mass activities above 6.3 Bq/kg were in the range 18–44 %, while the uncertainties of lower mass activities were in the range 52–110 %. The only exception was the sample from the R-1 sediment core at the depth 30–32 cm for which the uncertainty expressed for 2σ was 38 % although the mass activity was lower than 6.3 Bq/kg (5.1 ± 1.9 Bq/kg). Energy and resolution calibrations were performed by point sources of ¹⁰⁹Cd, ¹³⁷Cs (Canberra

Industries), and ⁶⁰Co (Amersham Buchler GmbH & CoKG). Efficiency calibration was performed by a sediment standard reference material of type CBSS 2 (Czech Metrological Institute). Quality control was performed by measuring an intercomparison soil reference material (Environmental Resource Associates, MRAD-11).

Dried until the constant weight, ground and homogenized sub-samples of the complete vertical profiles of all three sampling stations were subjected to determination of the CaCO₃ mass fraction. Analyses were performed according to the Austrian standard methods ÖNORM L1084 [29] using Scheibler calcimeter.

Grain-size analyses were performed on four selected sub-samples from the R-1 sediment core, three selected from the R-2 core, and on all 16 sub-samples from the R-3 core (Table 1). Selected sub-samples of the R-1 and R-2 sediment cores represent the uppermost parts, central parts, and the deepest parts of the cores. Sediment grain-size distribution was determined by Laser Diffraction Particle Size Analyzer (LS 13 320). Internationally accepted classification of sediments according to Folk [30] was used to classify the sub-samples.

Prior to the phase analysis, sediment was dried to the constant weight, ground, and homogenized. X-ray diffraction technique was used to determine the qualitative mineral phase composition of the sediment and it was applied on three composite samples from each sediment core. Phase determinations of the bulk samples were performed using a Philips X'pert powder diffractometer with CuKα radiation from the tube operating at 40 kV and 45 mA. An X-ray diffraction data set was collected from 4° to 63° 2θ.

Sedimentation rate was estimated from the undisturbed depth profiles of ¹³⁷Cs mass activities at the sampling stations R-1 and R-2. Well described method based on

Table 1 Selected sub-samples of the three sediment cores from the Vransko Lake subjected to the grain-size analysis

Sampling station	Sub-sample depth (cm)	Sub-sample	Sampling station	Sub-sample depth (cm)	Sub-sample
R-1	0–2.5	1	R-3	11–13	13
	17–18.5	2		13–15	14
	30–32	3		15–17	15
	40.5–41	4		17–19	16
R-2	0–3	5		19–21	17
	10–12	6		21–23	18
	18–20	7		23–25	19
R-3	0–3	8		25–27	20
	3–5	9		27–29	21
	5–7	10		29–31	22
	7–9	11		31–34	23
	9–11	12			

characteristic marker peaks or maxima of the ^{137}Cs mass activities representing sediment surfaces in 1964 and 1986 as well as the maximum depth at which ^{137}Cs was detected representing sediment surface in 1954 were used to estimate the sedimentation rate [1, 7, 31, 32]. The average sedimentation rate expressed in mm/a was estimated according to the equation (1):

$$v = \frac{d}{t_0 - t_{\text{ref}}}, \quad (1)$$

where d , expressed in mm, is the depth of ^{137}Cs mass activity peak or the maximum depth at which ^{137}Cs was detected, t_0 is the year of sampling and t_{ref} is the year associated with the ^{137}Cs mass activity peak or the maximum depth at which ^{137}Cs was detected.

Results and discussion

Sedimentation and source rocks

Results of the grain-size analysis are shown in the Fig. 2. Although the silt to sand ratio in different sub-samples was very variable, all sub-samples were classified as sandy silt with a mean grain size of 20–56 μm . The same sediment types at all three sampling stations indicate uniform sedimentation conditions in different parts of the lake. Considering the type of the sediment, the deposition environments can be regarded as the low- to medium-energy environments.

Mineral phase analysis showed the presence of calcite, quartz, micas, and pyrite in all three composite samples indicating the same source material for the whole lake. Such a mineral composition points to two different sources of the

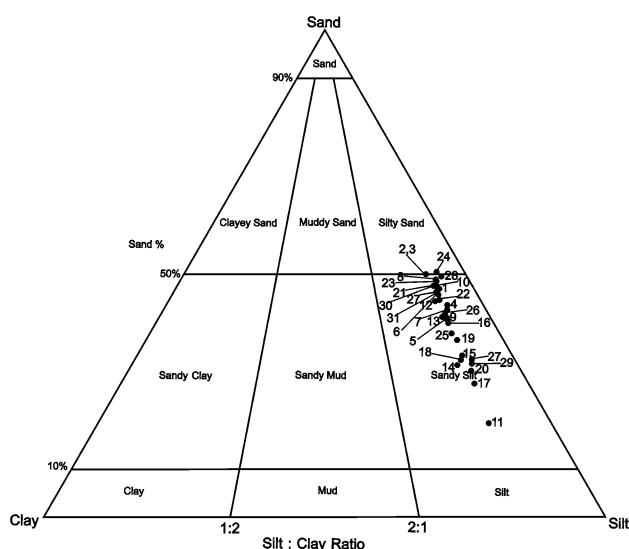


Fig. 2 Results of the grain-size analysis of the selected sub-samples of the R-1, R-2, and R-3 sediment cores

sediment closely related to the geological composition of the surrounding area comprising mainly carbonates, lacustrine deposits, and flysch. Similar mineral composition, with calcite and quartz as predominant minerals and with micas as subordinate to accessory minerals, was determined in surface sediments of the Kastela Bay and associated with terrigenous influence of the surrounding area [33]. Although the Kastela Bay is a marine environment and the Vransko Lake a freshwater environment, mineral composition of their sediments is comparable because it depends mostly on the geological composition of the area which is very similar in both areas, i.e. limestones and flysch are important geological members. Calcite represents the carbonate component of the sediments while quartz and micas represent the silicate/noncarbonate component. Calcite is a dominant mineral in limestones while quartz and micas are typical for noncarbonate layers of the flysch sequence. Quartz and micas can be considered as detrital minerals transported from the catchment area into the Vransko Lake. Calcite could also be of terrigenous/detrital origin considering the abundance of the limestones in the lake's surrounding area and the level to which the rocks are weathered. Part of the calcite could be of the biogenic origin contained in the lake organisms' shells. Although calcite could also be an authigenic mineral, its authigenic origin in the lake is not expected since the electrical conductivity of the lake water is lower than 0.13 mS/cm (Unpublished results) which is an unfavorable condition for precipitation [34]. It is presumed that pyrite in the lake sediments is authigenic in its origin. It implies the existence of the anoxic conditions in the sediment which could be a consequence of the enrichment with the organic residues [35–37]. Considering that the results of the grain-size analysis of the samples from this study suggested the existence of the low-energy depositional environments in the lake, accumulation of the organic matter would be possible, and is observed in the field prospection. The results of the mineral phase analysis point to the surrounding limestones, lacustrine deposits, and marls from the flysch sequence as the source rocks and to the physical weathering as the main process of sediment supply to the Vransko Lake.

Basic statistical parameters of CaCO_3 mass fractions in the R-1, R-2, and R-3 sediment cores are presented in Table 2 and depth profiles are shown in Fig. 3. CaCO_3 mass fractions at three studied sampling stations varied from 72 % to 94 % with the mean values in the range 82–88 %. High CaCO_3 mass fractions in sediments points to a significant influence of the surrounding carbonate rocks to the sediment composition. Sediments' carbonate component also originates partly from the flysch sequence although marl from the flysch is more important as a noncarbonate (silicate) material source for the lake sediments. Another source of the noncarbonate material are lacustrine deposits with a predominating silty loam located NW from the lake. This is in

agreement with the phase/chemical composition of the source rocks; mainly limestones from different stratigraphic units, flysch, and silty loam; in which CaCO₃ mass fractions of 95–99 %, 60–80 %, and approximately 15 %, respectively, were found [22]. From the results in the Table 2 and the Fig. 3 it is clear that the lowest CaCO₃ mass fractions are generally at the R-1 sampling station and that this station significantly differs from the other two. It is also visible from the Fig. 3 that the variation of the CaCO₃ mass fractions is the greatest in the R-1 sediment core. This could be explained by the position of the sampling station. This station is located in the northwest part of the lake where the influence of different source rocks is expected. Geological composition around this part of the lake is more heterogeneous than in the southeast part of the lake area. Rocks with more silicate component (less carbonate component) are more abundant in the northwest part of the lake area and lower CaCO₃ mass fractions are a consequence of the more pronounced influence of the flysch and lacustrine deposits. This implies that the composition of the lake sediment will vary according to the heterogeneity of the surrounding source rocks. Pronounced depth variations could be a result of the variable sediment input from the catchment area or from the watershed resulting in change of the carbonate/silicate sediment component ratio. The first significant change in the CaCO₃ depth profile at the R-1 station occurs at 23 cm depth when the mass fraction starts to decrease significantly towards the shallower parts of the profile. It points to an increased input of the terrigenous silicate material and/or to a decrease of the carbonate material input. Depth variation of the CaCO₃ mass fractions at the R-2 sampling station shows a similar pattern to the R-1 station although the variations are smaller. Here the mass fraction decrease towards the shallower sub-samples is observed at 17 cm depth. Station R-3 shows the most uniform depth distribution of the CaCO₃ mass fractions. This could imply that this part of the lake responds less to the changes in the composition of the lake’s input material.

Results of the radiometric analysis of ⁴⁰K, ²³²Th, and ¹³⁷Cs mass activities for the sampling stations R-1 and R-2

are presented in Table 3 and Fig. 3. ⁴⁰K mass activities vary in the range 31–166 Bq/kg with the mean values 99 Bq/kg at the R-1 station and 73 Bq/kg at the R-2 station. ²³²Th mass activities vary in a narrow range 3.1–18 Bq/kg with the mean values 11.0 Bq/kg and 6.4 Bq/kg for the R-1 and R-2 stations, respectively. Both, ⁴⁰K and ²³²Th mass activities are relatively low at both stations and are generally higher in the R-1 sediment core as it is shown in the Fig. 3. Low mass activities of these radionuclides are in accordance with the mainly carbonate sediment composition. Various authors determined ⁴⁰K and ²³²Th mass activities in the limestones in the ranges similar to this study: 1–160 Bq/kg for ⁴⁰K and 0–13.8 Bq/kg for ²³²Th [14, 17, 38–40]. Maximum ⁴⁰K and ²³²Th mass activities in the sediments of the Vransko Lake could be slightly elevated compared to these values due to the influence of the noncarbonate sediments or sediment components (i.e. noncarbonate minerals from the marl of the flysch series) of the source rocks. Tzortzis et al. [16] measured 187–434 Bq/kg of ⁴⁰K and determined the mean value of 16.1 Bq/kg for ²³²Th mass activity in the marl from Cyprus. These values are clearly higher than the values for the limestones. ¹³⁷Cs mass activities are relatively high at both stations and vary in the range 0.3–68 Bq/kg with the mean values 27 Bq/kg and 16 Bq/kg for the R-1 and R-2 stations, respectively. Such ¹³⁷Cs mass activities do not depend on the ⁴⁰K and ²³²Th mass activities since the later two are the natural radionuclides and ¹³⁷Cs is of anthropogenic origin and is unhomogeneously distributed in the environment [7]. However, once it is introduced in the environment, ¹³⁷Cs behaves almost identically as ⁴⁰K and very similar to ²³²Th. Close environmental behaviour of caesium and potassium is expected since these two elements are chemical homologues [41]. Although caesium is highly soluble and mobile [41], behaving as a conservative element, and thorium is mostly immobile and firmly bound to the particulate matter in the environment [42–44], behaving as a nonconservative element, their similar behaviour is expected in the water bodies with high particulate fluxes (e.g. coastal waters, lakes, rivers). In such waters rich with the particulate matter caesium is easily scavenged from the

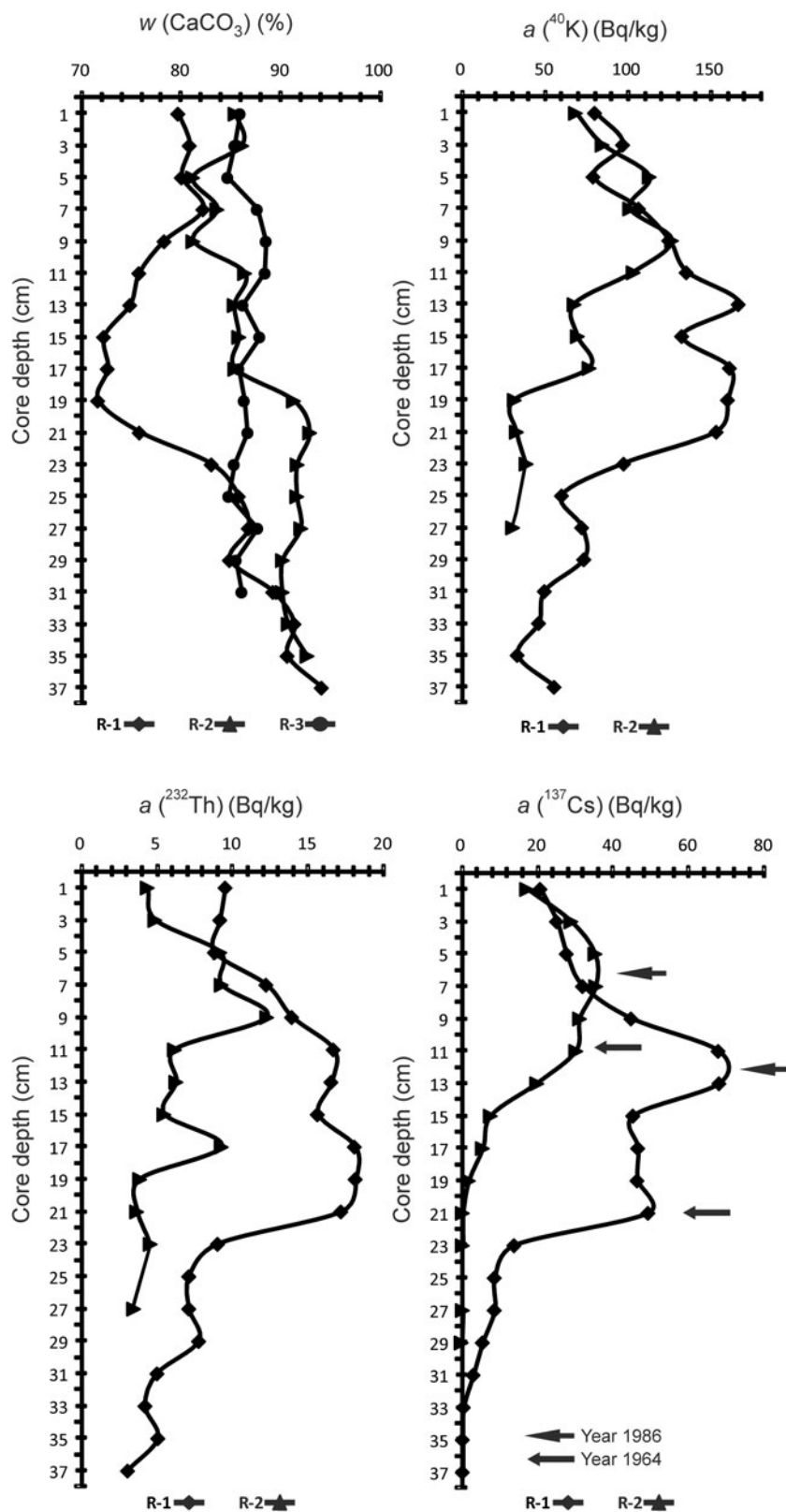
Table 2 Basic statistical parameters of CaCO₃ mass fractions in the R-1, R-2, and R-3 sediment cores

Core	Statistical parameter	CaCO ₃	Core	Statistical parameter	CaCO ₃	Core	Statistical parameter	CaCO ₃
R-1	N	19	R-2	N	18	R-3	N	16
	\bar{x}	82		\bar{x}	88		\bar{x}	86
	SD	6.8		SD	3.9		SD	1.2
	Minimum	72		Minimum	81		Minimum	85
	Maximum	94		Maximum	93		Maximum	88
	Median	81		Median	88		Median	86

CaCO₃ mass fractions are expressed in %

N number of results, \bar{x} mean value, SD standard deviation

Fig. 3 Depth profiles of CaCO_3 mass fractions at the R-1, R-2, and R-3 sampling stations and of ^{40}K , ^{232}Th , and ^{137}Cs mass activities at the R-1 and R-2 sampling stations



water column by sorption processes of caesium to the surface of the particles [45]. Therefore in the waters with high concentrations of the particulate matter both caesium and

thorium are preferably bound to the particle surfaces and removed from the water column to the bottom sediment. Thus, in this case caesium behaves as the nonconservative

element same as the thorium does. Close environmental behaviour of ^{40}K and ^{232}Th is clearly reflected in their depth profiles in the R-1 and R-2 sediment cores presented in the Fig. 3. They show almost identical profiles at the respective sampling stations. ^{40}K and ^{232}Th mass activities are generally higher at the R-1 station. Only in the upper 8–9 cm of the depth profiles the mass activities of the respective radionuclides are similar at both stations. The characteristic of all profiles in both sediment cores are lower mass activities in the upper 8 cm of the sediment and in the lower parts of the profiles. It is observed that the ^{40}K and ^{232}Th mass activities significantly increase from the 23 cm depth to the shallower sub-samples at the R-1 station and from the 17 cm depth at the R-2 station. The identical increase pattern of the mass activities of these two radionuclides suggests the increase of the terrigenous silicate material input into the lake. Clay minerals from the marl of the flysch sequence, lacustrine deposits, and soils are expected to be the source of ^{40}K . Flysch in the surrounding area is mainly composed of marl and potassium is normally associated with it [22, 46]. ^{232}Th also originates from the same silicate rocks or the silicate components since it is their constitutive element and is preferably bound to the sediment or soil particles. Since these radionuclides constitute or are preferably bound to the silicate minerals in sediments or soils, they can be considered as the indicators of the terrigenous influence of the silicate material. In accordance with it, they are generally transported to the lake in the particulate form. Depth profiles of ^{40}K and ^{232}Th mass activities show inverse patterns compared to the profiles of the CaCO_3 mass fractions. In the CaCO_3 mass fractions profiles significant changes also occur at the same depths of 23 cm for the R-1 sediment core and 17 cm for the R-2 core but here mass fractions decrease, opposite to the increase of the radionuclides mass activities. Lower CaCO_3 mass fractions at the R-1 sampling station compared to the R-2 station are in accordance with higher radionuclides mass activities at the R-1 station. Absolute or relative decrease of the CaCO_3 mass fractions observed above the 23 cm and 17 cm depth for the R-1 and R-2 stations, respectively, supports the increase of the terrigenous silicate influence to the lake sediment.

Caesium profiles at the R-1 and R-2 sampling stations show different characteristics. While mass activity peaks are clearly distinguishable in the R-1 profile, peaks in the R-2 profile are rather smooth and the maximum mass activity is approximately two times lower than in the R-1 profile. Smooth peaks with lower activities in the R-2 profile could point to the resuspension of the sediment, post-deposition diffusion and/or advection of ^{137}Cs or low sedimentation rate. Physical processes (resuspension and advection) are not supported by the ^{40}K and ^{232}Th profiles which are not smoothed like the ^{137}Cs profile. In case of the physical processes it would be expected for all profiles of the

Table 3 Basic statistical parameters of ^{40}K , ^{232}Th , and ^{137}Cs mass activities in the R-1 and R-2 sediment cores

Core	Statistical parameter	^{40}K	^{232}Th	^{137}Cs
R-1	N	19	19	19
	\bar{x}	99	11	27
	SD	43	5.1	23
	Minimum	34	3.1	0.3
	Maximum	166	18	68
	Median	97	9.2	25
R-2	N	13	13	13
	\bar{x}	73	6.4	16
	SD	32	2.8	14
	Minimum	31	3.5	0.3
	Maximum	126	12	36
	Median	70	5.5	17

Radionuclides mass activities are expressed in Bq/kg

N number of results, \bar{x} mean value, *SD* standard deviation

radionuclides bound to the sediment particles to be more or less equally smoothed. It is possible that the post-deposition diffusion of ^{137}Cs , but not of ^{40}K and ^{232}Th , occurred at the R-2 profile. Even in such a case the observed peaks are valid as chronomarkers because the maximum ^{137}Cs activities would still be contained in the sediment column at depths corresponding to the sediment surfaces of the years of the maximum ^{137}Cs input. Klaminder et al. [47] found that in spite of the ^{137}Cs post-deposition diffusion significant degradation of the 1986 peak in the fine grained varved lake sediment did not occur. It was also found that only a small fraction of ^{137}Cs in sediment of the North American lakes was mobile only in the first years after deposition and that it was rapidly immobilized [47]. According to some authors ^{137}Cs can potentially diffuse upwards and downwards, up to 2–4 cm, in the marine sediment column [48–50], while other authors concluded that caesium is strongly bound to particles and that its diffusion movement is negligible [48, 50, 51]. Low sedimentation rate at the R-2 sampling station would allow the input deposition material to be homogenized prior to sedimentation in the lake. This would cause the maximum ^{137}Cs activity in the input material to decrease. This is implied by the significantly lower ^{137}Cs mass activity representing the 1986 peak in the R-2 sediment core compared to the peak in the R-1 core.

Depth profiles of the CaCO_3 mass fractions and the radionuclides mass activities shown in the Fig. 3 point to the negative correlations between the CaCO_3 mass fractions and the studied radionuclides mass activities. Such interdependencies are confirmed by the results of the correlation analysis presented in Tables 4 and 5. High or very high negative correlations between the CaCO_3 mass fractions and the ^{40}K , ^{232}Th , and ^{137}Cs mass activities in both analysed sampling

cores are determined. At the R-1 station all three radionuclides mass activities show high or very high positive correlations with each other (Table 4). At the R-2 station positive correlations between ^{40}K and ^{232}Th and between ^{40}K and ^{137}Cs are high or very high while the correlation between ^{232}Th and ^{137}Cs is lower ($r = 0.64$) and is classified as the real significant correlation (Table 5). Such ^{137}Cs mass activities correlations show that ^{137}Cs is bound mostly to the noncarbonate particulate matter. Caesium is strongly absorbed on clay particles due to their high sorption property and its capability to exchange potassium ions in clay minerals [52, 53]. These results suggest that the main mechanism of the ^{137}Cs transport into the lake could be in the particulate form, where caesium is bound to the soil or sediment particles. However, if the ^{137}Cs would be transported into the lake in the dissolved form, it would be rapidly bound to the particles in the water column and deposited in the bottom sediment. The results in Tables 4 and 5 show that the correlations between the radionuclides mass activities are somewhat lower at the R-2 sampling station. This is attributed to the less emphasized influence of the terrigenous silicate material at this station which is suggested by the higher CaCO_3 mass fractions and the lower radionuclides mass activities (Tables 2, 3; Fig. 3).

Sedimentation rate

Maximum depth at which ^{137}Cs was detected in the R-1 and R-2 sediment cores was 31 cm and 19 cm, respectively (Fig. 3). Although the first release of ^{137}Cs into the environment was in the 1945, in this study the 1954 was used for the sedimentation rate estimation on the basis of the maximum depth of ^{137}Cs occurrence in the sediment profile because it was considered as the time of the first measurable ^{137}Cs input into the global environment [9]. Characteristic ^{137}Cs mass activities peaks representing the 1964 were observed at 21 cm depth in the R-1 sediment core and at 11 cm in the R-2 core (Fig. 3). Sedimentation rates for the 1954–1964 period of 10.0 mm/a at the R-1 sampling station and 8.0 mm/a at the R-2 station were estimated. One of the concerns when using maximum depth at which ^{137}Cs is detected for sedimentation rate estimation is the ^{137}Cs potential mobility in the sediment column due to diffusion and advection. Its mobility could lead to a downward shift of the first-onset horizon causing the ^{137}Cs occurrence at the depths greater than the depth at which it should be as the result of the atmospheric nuclear tests. Even if the ^{137}Cs redistribution to the lower parts of the sediment profiles in the Vransko Lake occurred, it can be concluded that in any case the sedimentation rate is not greater than 10.0 and 8.0 mm/a at the R-1 and R-2 sampling stations, respectively. Peaks representing the 1986 sediment surface were observed at 12 cm and 6 cm depth in the R-1 and R-2 sediment cores,

Table 4 Correlation matrix of ^{40}K , ^{232}Th , and ^{137}Cs mass activities and CaCO_3 mass fractions in sediment of the R-1 core in the Vransko Lake

	^{40}K	^{232}Th	^{137}Cs	CaCO_3
^{40}K	1.00			
^{232}Th	0.97	1.00		
^{137}Cs	0.93	0.94	1.00	
CaCO_3	-0.92	-0.95	-0.89	1.00

Marked correlations are significant at $p < 0.05$. $N = 19$

Table 5 Correlation matrix of ^{40}K , ^{232}Th , and ^{137}Cs mass activities and CaCO_3 mass fractions in sediment of the R-2 core in the Vransko Lake

	^{40}K	^{232}Th	^{137}Cs	CaCO_3
^{40}K	1.00			
^{232}Th	0.84	1.00		
^{137}Cs	0.91	0.64	1.00	
CaCO_3	-0.93	-0.83	-0.84	1.00

Marked correlations are significant at $p < 0.05$. $N = 13$

respectively (Fig. 3). Estimated sedimentation rates for the 1964–1986 period were 4.1 mm/a at the R-1 sampling station and 2.3 mm/a at the R-2 station. Estimated sedimentation rates for the 1986–2010 period were 5.0 mm/a and 2.5 mm/a at the R-1 and R-2 sampling stations, respectively. It is clear from these results that the sedimentation rates are higher at the R-1 sampling station in all three periods. Differences in sedimentation rates between these two areas were expected since the NW part of the lake is under higher influence of the lake watershed [21, 24]. Also, under the assumption that the first occurrence of ^{137}Cs in the depth profiles represents the sediment surface from the 1954, sedimentation rates at both sampling stations were significantly higher in the 1954–1964 period compared to the other two periods. It can be concluded that the sedimentation rate in the Vransko Lake varies in time and that it generally decreased after the 1964. The same pattern in the sedimentation rate variations was observed at both researched sampling stations pointing that the sedimentation changes affected the whole lake. Taking into account the observed increase of the silicate material input into the lake, it was also expected to observe the increase of the sedimentation rate contrary to the estimated decrease. This implies the greater importance of the carbonate source material to the sedimentation in the lake than suggested by the results in the Fig. 3.

Total estimated sedimentation rates from the 1954 to the 2010 were 5.5 mm/a at the R-1 station and 3.4 mm/a at the R-2 sampling station. Such estimations assume the uniform sedimentation rate which happens rarely in nature. Normally, several factors affect the sedimentation in any area

such as precipitation factor, inflow to the area and outflow from the area, reduction and/or oxidation conditions [1, 37]. Therefore, average sedimentation rates for the studied sampling stations were calculated. They were calculated as the arithmetic means of the sedimentation rates estimated for three periods. At the R-1 station average sedimentation rate of 6.4 mm/a was estimated and 4.2 mm/a at the R-2 station. Average sedimentation rates at both stations are higher than the total estimated sedimentation rates at the respective stations although the difference is not significant.

Conclusion

Sedimentation environment in the Vransko Lake is considered as the low- to medium-energy environment. It is likely that the anoxic conditions occur in the lake sediments. Sediment composition depends on the geological composition of the surrounding source rocks consisting mainly of limestones, lacustrine deposits, and flysch. Carbonate component predominates in the sediment composition. CaCO_3 mass fractions and ^{40}K and ^{232}Th mass activities vary with depth, i.e. the input of the carbonate and silicate deposition material into the lake is variable. Variability of the carbonate and silicate material input is reflected in the whole lake. It is presumed that all studied radionuclides are transported into the lake mainly in the particulate form. CaCO_3 mass fractions and the radionuclides mass activities are negatively correlated while the correlations between the radionuclides mass activities are positive. ^{40}K and ^{232}Th are indicators of the silicate material influence. Sedimentation rates are higher in the NW part of the lake in all three studied periods (i.e. 1954–1964, 1964–1986, and 1986–2010) probably due to the more pronounced watershed influence. Sedimentation rates showed the same patterns of the temporal variations and a general decrease after the 1964 at both studied sampling stations.

Acknowledgments This study was supported by the projects “Geochemical model of contaminants transport around waste disposal facilities” (119–0831529–1161) and “Radionuclides and trace elements in environmental systems” (098–0982934–2713) funded by the Ministry of Science, Education, and Sports of the Republic of Croatia. The authors are grateful to Mr. Robert Koscal for drawings. We would like to thank dr. sc. Delko Barisic from the Laboratory for Radioecology of the Rudjer Boskovic Institute for gamma-spectrometric measurements.

References

- Appleby PG (2002) Tracking environmental change using lake sediments. In: Last WM, Smol JP (eds) Chronostratigraphic Techniques in Recent Sediments, vol 1. Developments in Paleoenvironmental Research. Springer Netherlands, pp 171–203. doi:10.1007/0-306-47669-x_9
- Aygik G, Çetaku D, Erten H, Salihoglu I (2004) Dating of Black Sea sediments from Romanian coast using natural ^{210}Pb and fallout ^{137}Cs . J Radioanal Nucl Chem 259(1):177–180. doi:10.1023/b:jrmc.0000015825.67418.18
- Saxena DP, Joos P, Van Grieken R, Subramanian V (2002) Sedimentation rate of the floodplain sediments of the Yamuna river basin (tributary of the river Ganges, India) by using ^{210}Pb and ^{137}Cs techniques. J Radioanal Nucl Chem 251(3):399–408. doi:10.1023/a:1014821906600
- Ahn YS, Mizugaki S, Nakamura F, Nakamura Y (2006) Historical change in lake sedimentation in Lake Takkobu, Kushiro Mire, northern Japan over the last 300 years. Geomorphology 78(3–4):321–334. doi:10.1016/j.geomorph.2006.01.036
- Kumar B, Rai SP, Nachiappan RP, Kumar US, Singh S, Diwedi VK (2007) Sedimentation rate in North Indian lakes estimated using ^{137}Cs and ^{210}Pb dating techniques. Curr Sci 92:1416–1420
- Yao S, Li S, Zhang H (2008) ^{210}Pb and ^{137}Cs dating of sediments from Zigetang Lake, Tibetan Plateau. J Radioanal Nucl Chem 278(1):55–58. doi:10.1007/s10967-007-7191-2
- Mabit L, Benmansour M, Walling DE (2008) Comparative advantages and limitations of the fallout radionuclides ^{137}Cs , $^{210}\text{Pb}_{\text{ex}}$ and ^7Be for assessing soil erosion and sedimentation. J Environ Radioactiv 99(12):1799–1807. doi:10.1016/j.jenvrad.2008.08.009
- Ritchie JC, McHenry JR (1990) Application of radioactive fallout cesium-137 for measuring soil erosion and sediment accumulation rates and patterns: a review. J Environ Qual 19:215–233
- Zapata F (2003) Handbook for the Assessment of Soil Erosion and Sedimentation Using Environmental Radionuclides. Kluwer, Dordrecht
- Barišić D, Vertačnik A, Lulić S (1999) Caesium contamination and vertical distribution in undisturbed soils in Croatia. J Environ Radioactiv 46(3):361–374. doi:10.1016/s0265-931x(99)00011-9
- Lovrencic I, Barisic D, Orescanin V, Lulic S (2007) In situ determination of radon concentration and total gamma radiation in Kastel Gomilica, Croatia. Nucl Instr Meth in Phys Res B 263(1):186–190. doi:10.1016/j.nimb.2007.04.084
- Hirose K (2012) 2011 Fukushima Dai-ichi nuclear power plant accident: summary of regional radioactive deposition monitoring results. J Environ Radioactiv 111:13–17. doi:10.1016/j.jenvrad.2011.09.003
- Antovic N, Antovic I, Svrkota N (2010) Levels of Th-232 activity in the South Adriatic Sea marine environment of Montenegro. J Radioanal Nucl Chem 284(3):605–614. doi:10.1007/s10967-010-0512-x
- Tzortzis M, Tsertos H (2004) Determination of thorium, uranium and potassium elemental concentrations in surface soils in Cyprus. J Environ Radioactiv 77(3):325–338. doi:10.1016/j.jenvrad.2004.03.014
- Lovrencic I, Volner M, Barisic D, Popijac M, Kezic N, Seltkovic I, Lulic S (2008) Distribution of ^{137}Cs , ^{40}K and ^7Be in silver fir-tree (*Abies alba* L.) from Gorski Kotar, Croatia. J Radioanal Nucl Chem 275 (1):71–79. doi:10.1007/s10967-007-7009-2
- Tsabarlis C, Evangelidou N, Fillis-Tsirakis E, Sotiropoulou M, Patiris DL, Florou H (2012) Distribution of natural radioactivity in sediment cores from Amvrakikos Gulf (Western Greece) as a part of IAEA’s campaign in the Adriatic and Ionian Seas. Radiat Prot Dosim 150(4):474–487. doi:10.1093/rpd/ncr436
- Lima A, Albanese S, Cicchella D (2005) Geochemical baselines for the radioelements K, U, and Th in the Campania region, Italy: a comparison of stream-sediment geochemistry and gamma-ray surveys. 20(3):15
- Sakaguchi A, Yamamoto M, Sasaki K, Kashiwaya K (2006) Uranium and thorium isotope distribution in an offshore bottom sediment core of the Selenga Delta, Lake Baikal Siberia. J Paleolimnol 35(4):807–818. doi:10.1007/s10933-005-5621-0

19. Galindo C, Mougín L, Fakhri S, Nourreddine A, Lamghari A, Hannache H (2007) Distribution of naturally occurring radionuclides (U, Th) in Timahdit black shale (Morocco). *J Environ Radioactiv* 92(1):41–54. doi:10.1016/j.jenvrad.2006.09.005
20. Wan Mahmood Z, Ahmad Z, Adziz M, Mohamed C, Ishak A (2010) Radioactivity distribution of thorium in sediment core of the Sabah-Sarawak coast. *J Radioanal Nucl Chem* 285(2):365–372. doi:10.1007/s10967-010-0554-0
21. Fritz F (1984) Postanak i starost Vranskog jezera kod Biograda na moru [In Croatian]. *Geol Vjesnik* 37:231–243
22. Fritz F (1978) Hidrogeologija Ravnih Kotara i Bukovice [In Croatian]. *Krš Jugoslavije* 10(1):1–43
23. Fritz F (1977) Litostratigrafska i tektonska osnova hidrogeoloških odnosa Ravnih Kotara i Bukovice (Lithostratigraphical and tectonical framework to hydrogeology of Ravnih Kotara and Bukovica) [In Croatian]. University of Zagreb, Zagreb
24. Kapelj J (2002) Strukturni sklop šireg područja Promine u Sjevernoj Dalmaciji i odraz na hidrogeološke odnose [In Croatian]. University of Zagreb, Zagreb
25. Marković T, Miko S, Kapelj S, Buljan R, Larva O, Peh Z (2006) Behaviour of metals and nutrients in soils and groundwater of a karst polje. *J Geochem Explor* 88(1):124–129
26. Mamužić P (1966) Tumač Osnovne geološke karte SFRJ 1:100 000 za list Šibenik K 33–8 [Geology of the šibenik sheet, Basic Geological Map of SFRY 1:100 000—In Croatian]. Savezni geološki zavod, Beograd
27. Mamužić P, Nedela-Devide D (1973) Osnovna geološka karta SFRJ 1:100 000, list Biograd K 33–7 [Basic Geological Map of SFRY 1:100 000, Biograd sheet—In Croatian]. Savezni geološki zavod, Beograd
28. Mamužić P (1975) Osnovna geološka karta SFRJ 1:100 000, list Šibenik K 33–8 [Basic Geological Map of SFRY 1:100 000, Šibenik sheet—In Croatian]. Savezni geološki zavod, Beograd
29. ÖNORM L 1084 (1999) Chemische Bodenuntersuchungen—Bestimmung von Carbonat. Wien
30. Folk RL (1954) The distinction between grain size and mineral composition in sedimentary rock nomenclature. *J Geol* 62(4):344–359
31. Mizugaki S, Nakamura F, Araya T (2006) Using dendrogeomorphology and ^{137}Cs and ^{210}Pb radiochronology to estimate recent changes in sedimentation rates in Kushiro Mire, Northern Japan, resulting from land use change and river channelization. *Catena* 68(1):25–40. doi:10.1016/j.catena.2006.03.014
32. Al-Zamel AZ, Bou-Rabee F, Al-Sarawi MA, Olszewski M, Bem H (2006) Determination of the sediment deposition rates in the Kuwait Bay using ^{137}Cs and ^{210}Pb . *Nukleonika* 51(Supplement 2):S39–S44
33. Orescanin V, Barisic D, Lovrencic I, Mikelic L, Rozmaric-Macefat M, Pavlovic G, Lulic S (2005) The influence of fly and bottom ash deposition on the quality of Kastela Bay sediments. *Environ Geol* 49(1):53–64. doi:10.1007/s00254-005-0058-3
34. Wang YB, Liu XQ, Mischke S, Herzschuh U (2012) Environmental constraints on lake sediment mineral compositions from the Tibetan Plateau and implications for paleoenvironment reconstruction. *J Paleolimnol* 47(1):71–85. doi:10.1007/s10933-011-9549-2
35. Ogorelec B, Bole B, Leonidakis J, Cermelj B, Misic M, Faganelli J (2006) Recent Sediment of Lake Bled (NW Slovenia): sedimentological and Geochemical Properties. *Water Air Soil Pollut* 6(5–6):505–513. doi:10.1007/s11267-006-9034-5
36. Holmer M, Storkholm P (2001) Sulphate reduction and sulphur cycling in lake sediments: a review. *Freshwat Biol* 46(4):431–451. doi:10.1046/j.1365-2427.2001.00687.x
37. Schwörbel J (1987) Handbook of limnology. Ellis Horwood, New York
38. Brai M, Bellia S, Hauser S, Puccio P, Rizzo S, Basile S, Marrale M (2006) Correlation of radioactivity measurements, air kerma rates and geological features of Sicily. *Radiat Meas* 41(4):461–470. doi:10.1016/j.radmeas.2005.09.004
39. Gascoyne M (1982) Geochemistry of the actinides and their daughters. In: Ivanovich M, Harmon RS (eds) Uranium series disequilibrium: applications of environmental problems. Clarendon Press, Oxford, pp 33–55
40. UNSCEAR (1993) United Nations Scientific Committee on the Effects of Atomic Radiation Annex A: Exposures from natural sources of radiation. In: United Nations (ed) Sources and Effects of Ionizing Radiation, UNSCEAR 1993 Report to General Assembly, with Scientific Annexes. United Nations, New York, pp 34–89
41. Avery SV (1996) Fate of caesium in the environment: distribution between the abiotic and biotic components of aquatic and terrestrial ecosystems. *J Environ Radioactiv* 30(2):139–171. doi:10.1016/0265-931X(96)89276-9
42. Powell BA, Hughes LD, Soreefan AM, Falta D, Wall M, DeVol TA (2007) Elevated concentrations of primordial radionuclides in sediments from the Reedy River and surrounding creeks in Simpsonville South Carolina. *J Environ Radioactiv* 94(3):121–128. doi:10.1016/j.jenvrad.2006.12.013
43. Zhang L, Chen M, Yang W, Xing N, Li Y, Qiu Y, Huang Y (2004) Size-fractionated thorium isotopes (^{228}Th , ^{230}Th , ^{232}Th) in surface waters in the Jiulong River estuary China. *J Environ Radioactiv* 78(2):199–216. doi:10.1016/j.jenvrad.2004.05.004
44. van der Graaf ER, Koomans RL, Limburg J, de Vries K (2007) In situ radiometric mapping as a proxy of sediment contamination: assessment of the underlying geochemical and -physical principles. *Appl Radiat Isot* 65(5):619–633. doi:10.1016/j.apradiso.2006.11.004
45. Ilus E, Saxén R (2005) Accumulation of chernobyl-derived ^{137}Cs in bottom sediments of some finnish lakes. *J Environ Radioactiv* 82(2):199–221. doi:10.1016/j.jenvrad.2005.01.008
46. Aljinović D, Jurak V, Mileusnić M, Slovenec D, Presečki F (2010) The origin and composition of flysch deposits as an attribute to the excessive erosion of the Slani Potok Valley (“Salty Creek”). *Croatia Geol Croat* 3(63):312–322
47. Klaminder J, Appleby P, Crook P, Renberg I (2012) Post-deposition diffusion of ^{137}Cs in lake sediment: Implications for radiocaesium dating. *Sedimentology*. doi:10.1111/j.1365-3091.2012.01343.x
48. Sommerfield CK, Nittrouer CA (1999) Modern accumulation rates and a sediment budget for the Eel shelf: a flood-dominated depositional environment. *Mar Geol* 154(1–4):227–241. doi:10.1016/S0025-3227(98)00115-7
49. Zuo Z, Eisma D, Gieles R, Beks J (1997) Accumulation rates and sediment deposition in the northwestern Mediterranean. *Deep Sea Res Part II* 44(3–4):597–609. doi:10.1016/S0967-0645(96)00083-5
50. Pfitzner J, Brunskill G, Zagorskis I (2004) ^{137}Cs and excess ^{210}Pb deposition patterns in estuarine and marine sediment in the central region of the Great Barrier Reef Lagoon, north-eastern Australia. *J Environ Radioactiv* 76(1–2):81–102. doi:10.1016/j.jenvrad.2004.03.020
51. Gascó C, Antón MP, Pozuelo M, Meral J, González AM, Papucci C, Delfanti R (2002) Distributions of Pu, Am and Cs in margin sediments from the western Mediterranean (Spanish coast). *J Environ Radioactiv* 59(1):75–89. doi:10.1016/S0265-931X(01)00037-6
52. Petrincic B, Franic Z, Ilijanic N, Miko S, Strok M, Smodis B (2011) Estimation of sedimentation rate in the middle and south Adriatic Sea using ^{137}Cs . *Radiat Prot Dosim* 12:1–10
53. Lujanienė G, Beneš P, Štamberg K, Jokšas K, Vopalka D, Radžiūtė E, Šilobritienė B, Šapolaitė J (2010) Experimental study and modelling of ^{137}Cs sorption behaviour in the Baltic Sea and the Curonian Lagoon. *J Radioanal Nucl Chem* 286(2):361–366. doi:10.1007/s10967-010-0727-x